ELSEVIER

Contents lists available at ScienceDirect

Journal of Luminescence

journal homepage: www.elsevier.com/locate/jlumin



Optical properties of Ni-doped MgGa₂O₄ single crystals grown by floating zone method

Takenobu Suzuki*, Mark Hughes, Yasutake Ohishi

Research Center for Advanced Photon Technology, Toyota Technological Institute, 2-12-1, Hisakata, Tempaku-ku, Nagoya 468-8511, Japan

ARTICLE INFO

Article history:
Received 1 June 2009
Received in revised form
18 July 2009
Accepted 31 July 2009
Available online 8 August 2009

PACS: 78.40.Ha 78.55.Hx

Keywords: Ni-doped material Near-infrared emission

ABSTRACT

The single crystal growth conditions and spectroscopic characterization of Ni-doped MgGa $_2$ O $_4$ with inverse-spinel structure crystal family are described. Single crystals of this material have been grown by floating zone method. Ni-doped MgGa $_2$ O $_4$ single crystals have broadband fluorescence in the 1100–1600 nm wavelength range, 1.6 ms room temperature lifetime, 56% quantum efficiency and 1.05×10^{-21} cm 2 stimulated emission cross section at the emission peak. This new material is very promising for tunable laser applications covering the important optical communication and eye safe wavelength region

© 2009 Elsevier B.V. All rights reserved.

1. Introduction

The spectroscopy of Ni²⁺-doped optical materials has received much attention in recent years [1-5]. The initial and terminal states of the electronic transition are strongly coupled to the lattice phonon modes and the associated emission bandwidth becomes much broader than that of rare-earth ions such as Er³⁺, Nd³⁺ and Pr³⁺ and so on. Thus, the emission usually covers the wavelength range of 1100-1600 nm. Much of the present interest centers on the possibility of Ni²⁺-doped materials as active media for broadband optical amplifiers and tunable near-infrared laser systems. We discovered that MgGa2O4 was one of the most promising host materials for Ni²⁺. This is because Ni-doped MgGa₂O₄ has broadband near-infrared fluorescence, a long room temperature lifetime and a high quantum efficiency compared to other Ni-doped materials [6]. Ni-doped MgGa₂O₄ was well characterized for polycrystalline sintered bodies. However, single crystals of Ni-doped MgGa₂O₄ have not yet been grown and the optical properties were not known. In this paper, we present the crystal growth conditions and spectroscopic properties such as the refractive indices, absorption cross section, stimulated emission cross section, emission lifetime and quantum efficiency of Ni²⁺-doped MgGa₂O₄ single crystals prepared by the floating zone (FZ) method. These spectroscopic properties are necessary for the design of a laser system.

2. Experimental

Powders of MgCO $_3$ (Kojundo Kagaku Lab.: 3 N), Ga $_2$ O $_3$ (Kojundo Kagaku Lab.: 3 N) and NiO (Kojundo Kagaku Labs.: 3 N) were used as starting materials. The nominal compositions of the starting materials were MgCO $_3$:Ga $_2$ O $_3$:NiO = 0.99:1.05:0.01 and 0.90:1.05:0.10 (in mol) corresponding to Ni doping concentrations of 0.143 and 1.43 at%, respectively. A 5 mol% of Ga $_2$ O $_3$ in excess of the stoichiometric compositions was added to compensate for evaporation of Ga $_2$ O $_3$ during the FZ process.

The 100 g batches were mixed in an alumina mortar, and then calcined at 1300 °C for 1 h in air. After grinding with 1 wt% polyvinyl alcohol, the powder was rubber-pressed under a hydrostatic pressure of 100 MPa and a round molded specimen was prepared. The molded specimen was sintered at 1200 °C for 2 h in air. The typical dimension of the sintered seed and feed rod was 5–8 mm in diameter and 100–150 mm in length.

The growth apparatus used was an image furnace with double ellipsoidal mirrors (Canon Machinery), in which two 650 W halogen lamps were used as a heat source. Crystal growth was performed in the typical manner of the floating zone method. The crystal growth rate was 1–10 mm/h. The rotation rates of feed rod and seed crystal were 30 rpm. The atmosphere was controlled by flowing dry oxygen at rates of 1–5 l/min.

^{*} Corresponding author.

E-mail address: takenobu@toyota-ti.ac.jp (T. Suzuki).

The grown crystals were cut perpendicularly to the growth direction, and then the cut surfaces were optically polished. The crystal phases of the sample were evaluated in an X-ray diffract meter (Shimadzu, XRD-600) using Cu K α radiation. The chemical compositions were analyzed by an energy dispersive X-ray (EDX) spectrometer (JED-2300, JEOL) attached to a scanning electron microscope (JSM-6490A, JEOL).

Optical absorption spectra were recorded by a double-beam monochromator (Lambda900, Perkin-Elmer) over a range of 175-3300 nm. Fluorescence from the sample excited by a 974 nm laser diode was dispersed by a single monochromator with a diffraction gratings blazed at 1000 nm and detected by a near-infrared photomultiplier tube (Hamamatsu Photonics, H9170-75). The monochromator was purged with N2 gas to reduce absorption of near-infrared fluorescence by moisture in the air. The decay curve of the emission was obtained by a digital oscilloscope (Yokogawa, DL-1620) and the fluorescence lifetime was taken from the 1/e fall time of the curve. The samples were cooled from 300 to 5 K by a cryostat (Daikin) and heated by a resistance heater to about 500 K. Quantum efficiency (QE) measurements were taken with the same system used for spectral measurements except samples were placed in an integrating sphere (Labsphere, 4P-GPS-040-SF), and the signal was detected with an InGaAs detector (Hamamatsu photonics, G5852-11). The samples were mounted behind a baffle such that there was no direct line-of-sight between the sample and the exit port, and angled such that reflected excitation light was directed away from the entrance port. The number of photons absorbed was taken to be proportional to the difference between the area under the corrected laser line spectrum with the sample present $(I_{sample}(\lambda))$ and without the sample present $(I_{sphere}(\lambda))$. The number of photons emitted was taken to be proportional to the area under the corrected emission spectrum ($I_{PI}(\lambda)$). The spectra were corrected with a correction spectrum $(C(\lambda))$ and for the photon energy by multiplying by the wavelength, since a higher photon flux is required at longer wavelengths to produce the same irradiance per unit area. Hence the quantum efficiency (η_{OE}) was calculated using the following equation:

$$\eta_{QE} = \frac{\int \lambda I_{PL}(\lambda)C(\lambda)d\lambda}{\int \lambda I_{sphere}(\lambda)C(\lambda)d\lambda - \int \lambda I_{sample}(\lambda)C(\lambda)d\lambda}$$
(1)

3. Struck and Fonger analysis of emission lifetime

The Struck–Fonger (S–F) analysis gives the effective phonon energy, the number of phonons, the Huang–Rhys factor and the radiative emission lifetime from the temperature dependence of

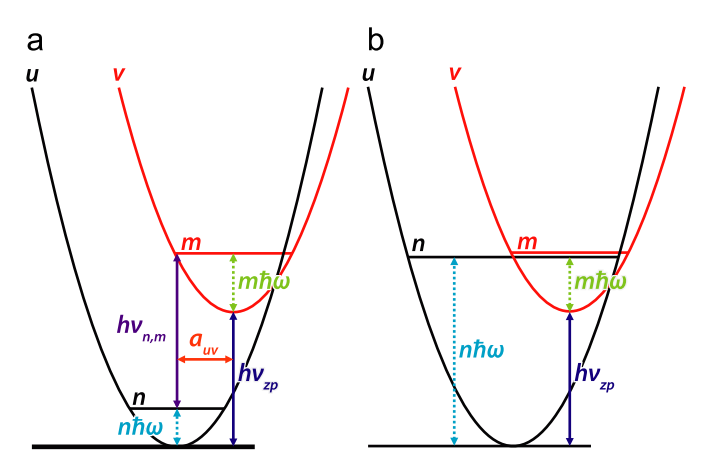


Fig. 1. Energy balances of (a) radiative transition (Eq. (2)) and (b) non-radiative transition (Eq. (3)).

the measured emission lifetime [7] and can be used to estimate the ratio of radiative and non-radiative relaxation rates of emission centers in solids. When the radiative and non-radiative transition energy balances are

$$hv_{zp} + m\hbar\omega - n\hbar\omega - hv_{n,m} = 0$$
 (2)

[Fig. 1(a)] and

$$hv_{zp} + m\hbar\omega - n\hbar\omega = 0 \tag{3}$$

[Fig. 1(b)] where hv_{zp} is the zero-phonon energy, $hv_{n,m}$ is the photon energy, $\hbar\omega$ is the effective phonon energy, and n and m are the number of phonons associated with the transitions from the ground electronic state and the excited electronic state, respectively. The relations expressed in these equations are illustrated in Fig. 1. The radiative lifetime of the emission can be calculated using [7]

$$\tau_{calc} = \frac{1}{R_{uv} + N_{uv}W_{p_u}} \tag{4}$$

where $p_u=n-m$ (thus $hv_{zp}=p_u\hbar\omega$), R_{uv} and N_{uv} are constants from the electronic portion of the integral of the radiative and non-radiative transition and W_{p_u} is the thermal Franck-Condon weight, which is given by

$$W_{p_u} = \sum_{m = \max(0, -p_u)} (1 - r_v) r_v^m \langle u_{p_u + m} | v_m \rangle^2$$
 (5)

where $r_v = \exp(-\hbar \omega/kT)$ and $\langle u_{p_u+m}|v_m\rangle^2$ is the overlap integral of the initial and final states. The overlap integrals are calculated by recursion formula given by Manneback:

$$\langle u_0|v_0\rangle = \exp(-\frac{1}{8}a_{uv}^2),\tag{6}$$

$$\langle u_n | v_{m+1} \rangle = \frac{1}{\sqrt{m+1}} \left(\frac{1}{2} \langle u_n | v_m \rangle + \sqrt{n} \langle u_{n-1} | v_m \rangle \right) \tag{7}$$

and

$$\langle u_{n+1}|v_m\rangle = \frac{1}{\sqrt{n+1}} \left(\frac{1}{2} \langle u_n|v_m\rangle + \sqrt{m} \langle u_n|v_{m-1}\rangle\right) \tag{8}$$

where a_{uv} is the offset of the parabolas of the ground state and the excited state as shown in Fig. 1(a). The summed difference lifetime $\Delta \tau$ given by

$$\Delta \tau = \frac{\sqrt{\sum (\tau_{meas} - \tau_{calc})^2}}{N - 4} \tag{9}$$

where N is the number of the measured temperatures, was minimized to get a optimized set of R_{uv} , a_{uv} , $\hbar \omega$ and p_u . N_{uv} was assumed to be a constant of $10^{13} \, \mathrm{s}^{-1}$ which is the same those reported in Refs. [11–13].

4. Results and discussion

Fig. 2 shows a photograph of a Ni-doped MgGa₂O₄ single crystal. Bubble and inclusion-free crystals were obtained with a growth rate of less than 5 mm/h and an oxygen flow of more than 5 l/min. Although the growth rate of 5 mm/h was relatively high compared to the usual FZ process, the quality, especially uniformity of the color, of the single crystal grown at 5 mm/h was better than single crystals grown at lower rates. The higher

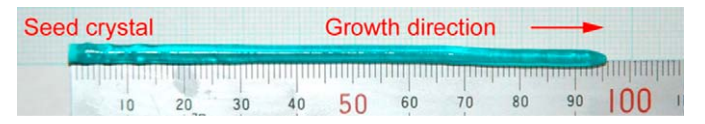


Fig. 2. Photograph of Ni-doped MgGa₂O₄.

Download English Version:

https://daneshyari.com/en/article/5402877

Download Persian Version:

https://daneshyari.com/article/5402877

Daneshyari.com